Materials Today Bio 31 (2025) 101567

Contents lists available at ScienceDirect

Materials Today Bio

journal homepage: www.journals.elsevier.com/materials-today-bio

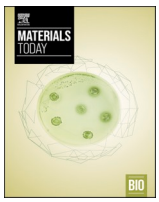

Nano-adjuvant based on lipo-imiquimod self-assembly for enhanced foot-and-mouth disease virus vaccine immune responses *via* intradermal immunization

Wenzhu Yin [a,c,*], Zeyu Xu [b], Fang Ma [a], Bihua Deng [a,c], Yanhong Zhao [a,b], Xiaoxin Zuo [a], Haiyan Wang [a], Yu Lu [a,b,**]

[a] *Institute of Veterinary Immunology & Engineering, Jiangsu Academy of Agricultural Sciences, Nanjing, 210014, China*
[b] *College of Veterinary Medicine, Nanjing Agricultural University, Nanjing, 210095, China*
[c] *GuoTai (Taizhou) Center of Technology Innovation for Veterinary Biologicals, Taizhou, 225300, China*

ARTICLE INFO

Keywords:
Imiquimod
Lipidation
Self-assembly
Nano-adjuvant
Intradermal immunity
Foot-and-mouth vaccine

ABSTRACT

Excellent adjuvants and proper immunization routes play pivotal roles in activating a robust immune response. Nano-adjuvants have the advantages of enhancing immunogenicity, targeting delivery, and improving stability to provide a new solution for vaccine delivery. In this work, we designed and synthesized a pro-immunostimulant of liposolubility imiquimod derivative IMQP, which was synthesized by reaction of palmitoyl chloride with parent imiquimod (IMQ). Using an inactivated foot-and-mouth disease virus (FMDV) as antigen, and the as-synthesized IMQP containing long carbon chain as nano-adjuvant, we formulated a self-assembled foot-and-mouth disease nano-vaccine (IMQP@FMDV) by re-precipitation method for intradermal (I.D.) immunity vaccination. Because of its small size (~131.75 ± 41.70 nm) and fat-soluble, the as-fabricated lipid nanoparticles (LNPs) showed promising potential for efficient delivery of antigens to immune cells. Also, lysosomal escape was confirmed by co-localization dendritic cells (DCs). Our findings demonstrated that IMQP nano-adjuvant greatly promoted the expression and secretion of cytokines and chemokines with a balance Th1/Th2 immune response *via* the I.D. administration. Meanwhile, due to the slowly releasing of IMQ by the hydrolysis of IMQP, IMQP persistently stimulated antigen-presenting cells (APCs) maturation and promoted antigen presentation, and subsequently induced the activation of the related downstream NF-κB and MAPK pathways of the TLR7 signaling pathway, thereby stimulated a robust both humoral and cellular immune response.

1. Introduction

Foot-and-mouth disease (FMD), a highly infectious and significant economic concern illness, is a main virus disease of cloven-hoofed animals [1,2]. Routine immunization is one of the preferred methods for combating the disease in endemic nations. Especially, addition of adjuvants and alternative delivery methods are utilized to reduce the required dose of FMD vaccine, boost immune response, and improve vaccination efficacy.

Currently, commercially available FMD vaccines are formulated by combining inactive whole viruses and aluminium gel or mineral oil adjuvants. The Toll-like receptor (TLR) agonists as the potent stimulants of an innate immune system hold promises for applications in vaccine adjuvants because of their strong activation of antigen-presenting cells (APCs) [3]. Particularly, TLR7 agonists can boost T-helper (Th) 1-type immune responses, improve cross-presentation capacity, and activate MyD88-dependent signaling in innate immunity cells, which is accompanied by increasing expression of pro-inflammatory cytokines and co-stimulatory molecules [4–8]. Among them, imiquimod (IMQ), a commercialized TLR7 agonist, has been used as an adjuvant for formulating various vaccines. However, due to its insolubility and poor pharmacokinetics, IMQ limited for injection vaccine. Lipidation is an important modification strategy for bioactive molecules, which has shown exceptional promise in pharmaceutical applications [9–12]. Various researches demonstrate that the combination of lipid alkyl chain groups or the formation of liposomes with TLR agonists can effectively

* Corresponding author. Institute of Veterinary Immunology & Engineering, Jiangsu Academy of Agricultural Sciences, Nanjing, 210014, China.
** Corresponding author. Institute of Veterinary Immunology & Engineering, Jiangsu Academy of Agricultural Sciences, Nanjing, 210014, China.
E-mail addresses: 20170023@jaas.ac.cn (W. Yin), luyu201710@163.com (Y. Lu).

https://doi.org/10.1016/j.mtbio.2025.101567
Received 1 January 2025; Received in revised form 1 February 2025; Accepted 8 February 2025
Available online 12 February 2025

improve the pharmacokinetic profile *via* slow dissemination from the injection site without systemic toxicity [9,12]. In addition, lipidation can enhance the targeting transportation ability of lymph nodes (LNs), leading to dramatic increases in T-cell priming [13,14]. Inspired by these excellent results in literature, in order to enhance lipid solubility and reduce the dispersion rate of small molecule IMQ *in vivo*, in this contribution, we incorporated palmitoyl to IMQ through typically amidation reaction to synthesize a lipidation IMQ derivative IMQP, which enhanced the membrane permeability of parent IMQ, and sequentially improved the cellular and immune response of inactive FMD vaccine.

Meanwhile, it is worth mentioning that the proper administration route plays a vital role in activating a robust immune response also. As everyone knows, the skin is the biggest organ in the animal body and the most common site of immune injection, because skin has various rich immune system cells, including Langerhans cells (LCs), mast cells, macrophages, T cells, and dendritic cells (DCs) etc. Many researches indicted that I.D. vaccination elicited a robust and prolonged antibody response compared with intramuscular (I.M.) vaccination. Despite I.D. route could improve vaccine immunogenicity, however the degree of improvement was still relatively weak. Thereby, incorporation of new adjuvants into vaccine is expected to further improve vaccine efficacy and spares more vaccine doses [15]. Recently, there has been growing interest in nanoparticle-based delivery systems aimed at boosting antigen delivery efficiency and immunogenicity [16]. Nanoparticles (NPs)-mediated synchronous delivery of adjuvant and antigen emerges as a promising strategy to enhance APCs uptake and reduces systemic side effects [9]. Among these, self-assembled lipid nanoparticles (LNPs) with varying sizes, shapes, and surface properties have garnered considerable attention since they share better cellular uptake capacity in target cells in *vitro* and in *vivo* [17]. LNPs are the most clinically advanced non-viral delivery technology among the numerous nanocarrier options that have been investigated for nucleic acid delivery. However, the development of clinically relevant LNP formulations has been far from straightforward. Accordingly, in this work, we used the as-synthesized lipid IMQP and FMD antigen to construct IMQP@FMDV LNPs by re-precipitation method. With the as-fabricated FMD nano-vaccine in hands, we investigated the immune synergism of combing the novel TLR7 against-based adjuvant with I.D. delivery.

In our strategy, the results suggested that IMQP@FMDV nano-vaccine could recruit a large number of APCs with a good biological safety using I.D. injection. The APCs were activated to secrete amounts of pro-inflammatory cytokines, like IFN-γ, TNF-α, and IL-6. Subsequently, IMQP activated $CD4^+$ and $CD8^+$ T cells through antigen presentation, and continuously stimulated the body to produce IgG antibodies as well as humoral and cellular dual immune response. Meanwhile, we also used mutual validation to explore the immune enhancement mechanism of IMQP through molecular docking, RT-qPCR, Western-Blot and RNA-sequencing (RNA-seq). Our findings exhibited that IMQP enhanced immune efficiency through TLR7/MyD88/NF-κB and MAPK signaling pathways (Scheme 1). In summary, our results provided a proof-of-concept for IMQP as a vaccine adjuvant against virus inflection diseases.

2. Results and discussion

2.1. Characterization, solubility and safety of IMQP and IMQP@FMDV nano-vaccine

Size of NPs, which was less than 200 nm, endowed these materials with a high biocompatibility and effective cell uptake. Using OVA as model antigen, we prepared the IMQP@OVA LNPs through re-precipitation method for investigating the nanostructure and loading capability. In addition, using inactivated FMDV instead of OVA, we formulated an IMQP@FMDV nano-vaccine for evaluation of the immune potency. As shown in Fig. 1a and b, the IMQP NPs possess negative charged, and the ζ potential was −15.03 ± 1.08 mV, which is in agreement with previous report [9]. Moreover, its hydrodynamic particle mean diameter (HPD) was about 127.73 nm with a PDI 0.128.

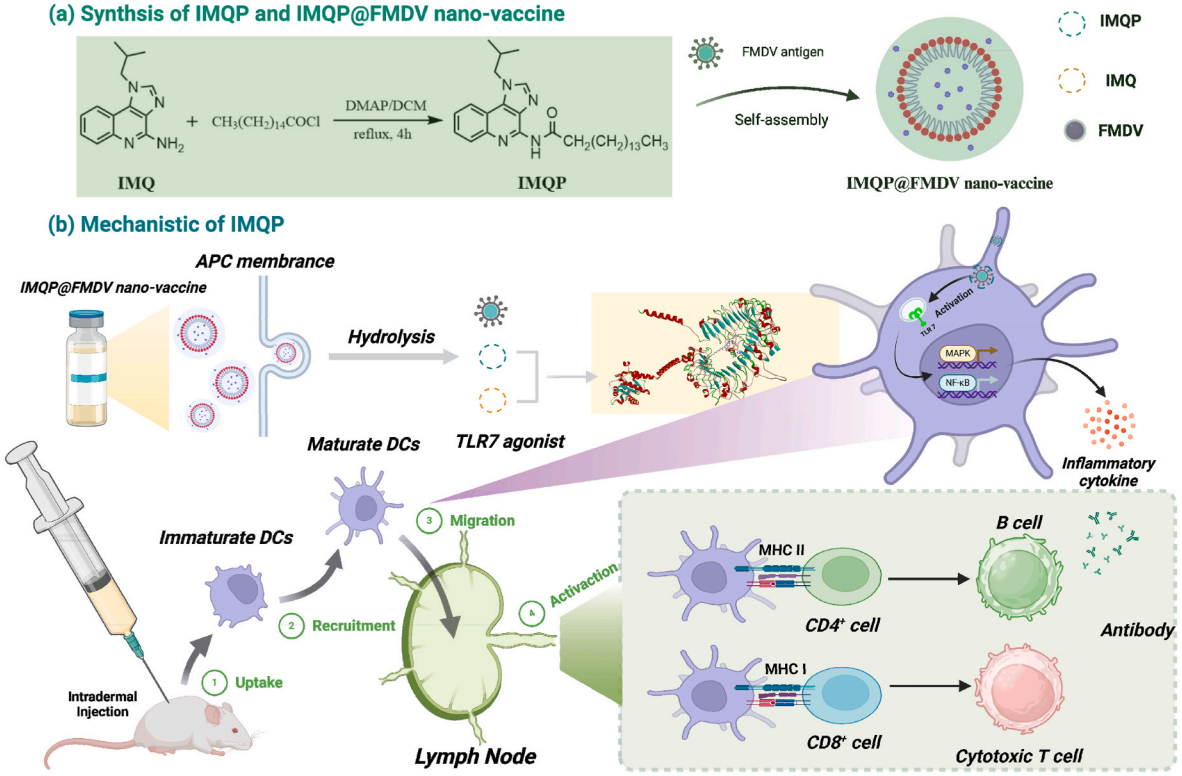

Scheme 1. The Schematic representation of (a) the synthesis of IMQP and (b) proposed *in vivo* immune response through TLR7/MyD88-dependent NF-κB and MAPK signaling pathways.

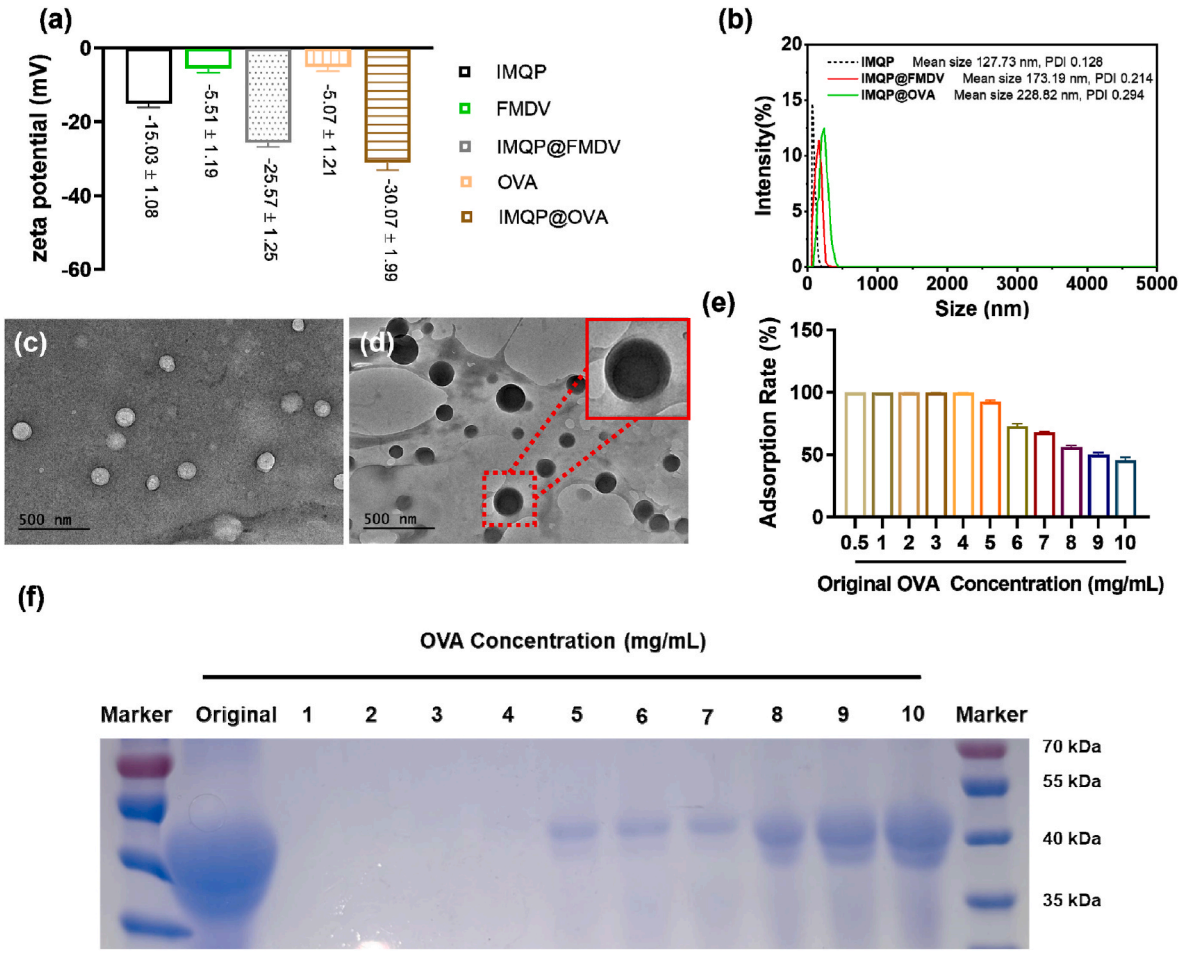

Fig. 1. The characterization of IMQP. The ζ potential (a) and DLS (b) of IMQP, IMQP@FMDV and IMQP@OVA LNPs. TEM images of (c) IMQP NPs and (d) IMQP@OVA LNPs. (e) The adsorption rate of IMQP load OVA by BCA kit. (f) SDS-PAGE of the supernatant of OVA. All data were expressed as means ± SD, n = 3.

IMQP@FMDV and IMQP@OVA LNPs displayed a negative ζ potential (−25.57 ± 1.25 and −31.06 ± 1.99 mV, respectively), but was more negative than IMQP NPs. Similarly, the HPD of 173.19 and 228.82 nm with polydispersity indices (PDI) of 0.214and 0.294, respectively. The increased particle size and PDI could be attributed to complex FMDV or OVA.

Transmission electron microscopy (TEM) investigations were carried out to provide further insights into the morphology of the as-prepared IMQP and IMQP@OVA LNPs structures (Fig. 1c and d). Compared with the IMQP NPs and IMQP@OVA LNPs displayed a "core-shell" nanostructure, which was attributed to OVA wrapping on the surface of IMQP NPs (seeing the enlarged image in Fig. 2d). The mean diameter between IMQP NPs and IMQP@OVA NPs increase slightly, from 118.97 ± 16.02 to 131.75 ± 41.70 nm, and the data were in accordance with the DLS results. Self-assembly is an attractive bottom-up approach to complex architectures and nanomaterials [18]. The method was simple, effective, and cost-effective for large-scale production. Our as-synthesized IMQP possessed an amphiphilic structure, characterized by a hydrophilic IMQ head and a long hydrophobic alkyl chain. This unique property endowed IMQP molecule with self-assembly to form nanostructures when mixed with poor solvent water. When IMQP in DMF solution was added into poor solvent water, the dissolved IMQP inside DMF precipitated through self-assembled to generate NPs duo to poor solubility of IMQP in water. The driving force of self-assembly mainly consists of hydrogen bonding, dipole-dipole forces, hydrophobic effect, π-π weak interactions with the precipitation of IMQP in the poor solvent water [19]. In addition, in the water system, hydrophilic part occupies on the surface of nanoparticles, which further interacts with OVA by H-bond and dipole-dipole to form "core-shell" nanostructure [20].

The ζ potential, DLS and TEM results all indicated that the IMQP loaded OVA successfully. With the findings of BCA protein assay kit, it was found that the maximum adsorption capacity of IMQP to OVA was 455.33 ± 16.92 mg/g (Fig. 1e). In addition, SDS-PAGE (Fig. 1f) image of OVA residue in the supernatant after IMQP loading OVA also confirmed that IMQP self-assembled with antigen to form lipid NPs. Additionally, OVA labeled with Rhodamine B (OVA-Rh B) also self-assembled with IMQP to construct NPs for examination NPs size and loading ability. From confocal scanning microscope (CLSM) images (Fig. 1), it can be seen that small particles (bright field), red fluorescent dots and they can overlap completely. This analysis can be verified that IMQP adsorbs OVA to self-form IMQP@OVA LNPs.

The solubility of IMQP is closely related to the route of administration. Numerous of literature have proved that the exceptional lipid solubility of adjuvant can improve cell membrane permeability and subsequently induce robust cellular immunity. Moreover, lipidation TLR7 agonists can reduce their systemic side effects in the immune process. As shown in Table 1, our IMQP showed excellent solubility in different solvents such as DMSO, EtOH, W/O/W emulsion (ISA201, ISA206) and mineral oil. The results demonstrated that IMQP could be used as an injectable formulation and amenable to co-formulation in a number of different lipid and oil-based adjuvants.

The safety and toxic issues of adjuvants are the key attention to their potentials. We firstly used CCK-8 to evaluate the biocompatibility of IMQP. The results (Fig. 2a) showed that the cell viability of RAW264.7 cells were greater than 80 % when the concentration of IMQP was up

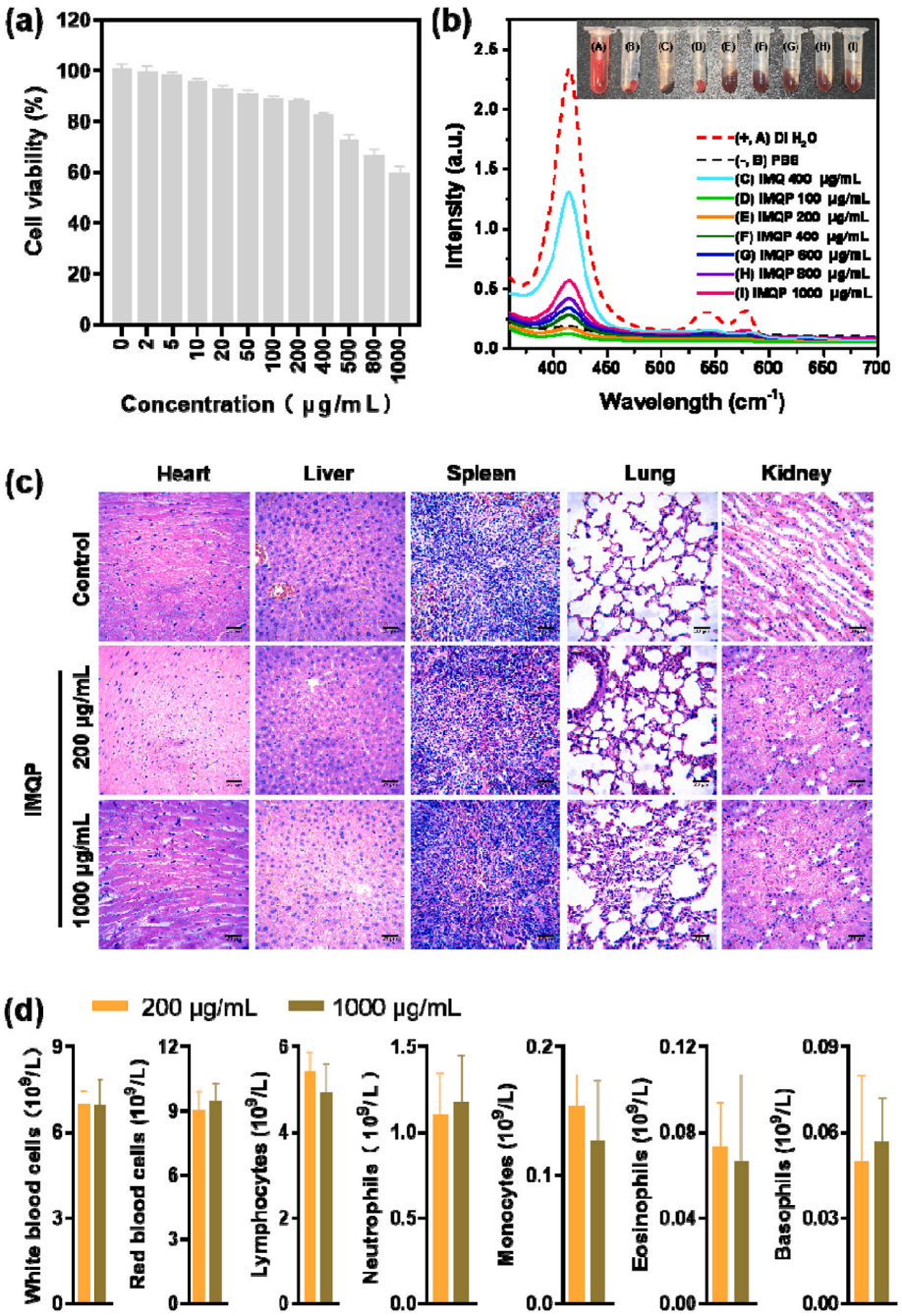

Fig. 2. Biosatety of IMQP. (a) The CCK-8 result with RAW 264.7 cells. (b) The hemolysis test by 1 % RBCs of SPF chicken. Inset: the optical photos of co-incubation of RBCs with IMQP (c) The H&E staining of IMQP with different concentrations (200 μg/mL, 1000 μg/mL). Scale bar: 20 μm. And (d) the complete Blood Count. The following parameters were measured: white blood cells, red blood cells, lymphocytes, neutrophils, monocytes, eosinophils and basophils. All blood analysis data fell well within the normal ranges. Results were expressed as means ± SD, n = 3.

Table 1
The maximum solubility of IMQP in different solvents in room temperature.

Sovlent	Mineral Oil	ISA201	ISA206	EtOH	DMF	DMSO	EA	DCM
Maximum solubility (mg/mL)	19	2.9	2.7	2.1	5.2	3.3	12	36

400 μg/mL, indicating its low cytotoxicity in injection concentration. Then, we examined the biosafety of IMQP *in vitro* by carrying out hemolysis test. As illustrated in Fig. 2b, when the concentration of IMQP was increased to 1000 μg/mL, the corresponding hemolysis rate was just about 13.93 %. However, the pristine IMQ was about 37.55 % at 50 μg/mL (corresponding to 100 μg/mL IMQP in the same molar concentration), which suggesting the IMQP exhibited better biocompatibility than IMQ. Moreover, the optical photographs (insert of enlarged image in Fig. 2b) also visually confirmed that IMQP activation did not cause hemolysis behavior of RBCs. In the same time, we also observed that the RBCs with IMQ had atrophy and structural changes, however most of the red blood cells still maintain normal morphology

without atrophy, membrane rupture and other phenomena when the concentration of IMQP was at 1000 μg/mL (Fig. S2). In brief, IMQP can be used alone or co-combination with else oil-based adjuvants in a range of concentration as an injection dosage.

Hematological and histological analyses of vaccinated mice were performed to further investigate the impact of IMQP *in vivo*. First, we evaluated the major organs such as heart, liver, spleen, lung, and kidney by H&E staining. After I.P. injection of low (200 μg/mL) and high (1000 μg/mL) concentrations of IMQP in mice, these organ tissues still kept normal histological structures without significant inflammation or injury comparing with negative control group (Fig. 2c). Furthermore, the mice were subjected to a hematology analysis after 7 days of administration. The important parameters, such as white blood cells (WBCs), RBCs, lymphocytes, neutrophiles and so on, were collected. As seen in Fig. 2d, the indexes of all blood analysis data fell well within the normal range. Considering the practical applications, we investigated the endotoxin (ET) concentration of IMQP (200 μg/mL) using the endotoxin detection kit, and results showed that the value of ET was below 2.5 EU/mL. Overall, these findings demonstrated that the IMQP was safe as potential vaccine adjuvant.

2.2. Recruitment and activation of immune cells at injection site

In order to initiate systemic immunity, it was necessary that antigen was uptake by APCs at the injection site, where then transferred into lymphocytes to generate immune responses. Notably, after I.D. administration, LCs in the epidermis were stimulated by vaccine and then migrated to the draining lymph nodes (DLNs) to activate T lymphocytes for exerting immune effects. Therefore, I.D. immunization had many advantages compared with I.M. injection. H&E analysis demonstrated that pure FMDV by I.D. injection caused no inflammatory response within 1–7 days, which was similar to I.M. inoculation with IMQP@FMDV nano-vaccine (IMQP@FMDV-IM) (Fig. 3a). However, the adjuvant groups, such as 201@FMDV-ID and IMQP@FMDV-ID groups, when used I.D. injection, showed the phenomenon of inflammatory cells, which neutrophils and phagocytes were infiltrated in the dermis and around the sebaceous glands on 1 dpi. In particular, the IMQP@FMDV-ID group also caused obvious injection site reactions due to the adjuvant effect of IMQP *via* I.D. injection. It was worth noting that only IMQP@FMDV-ID group maintained the recruitment of inflammatory cells after 7 days. So, we speculated that the IMQP could durably

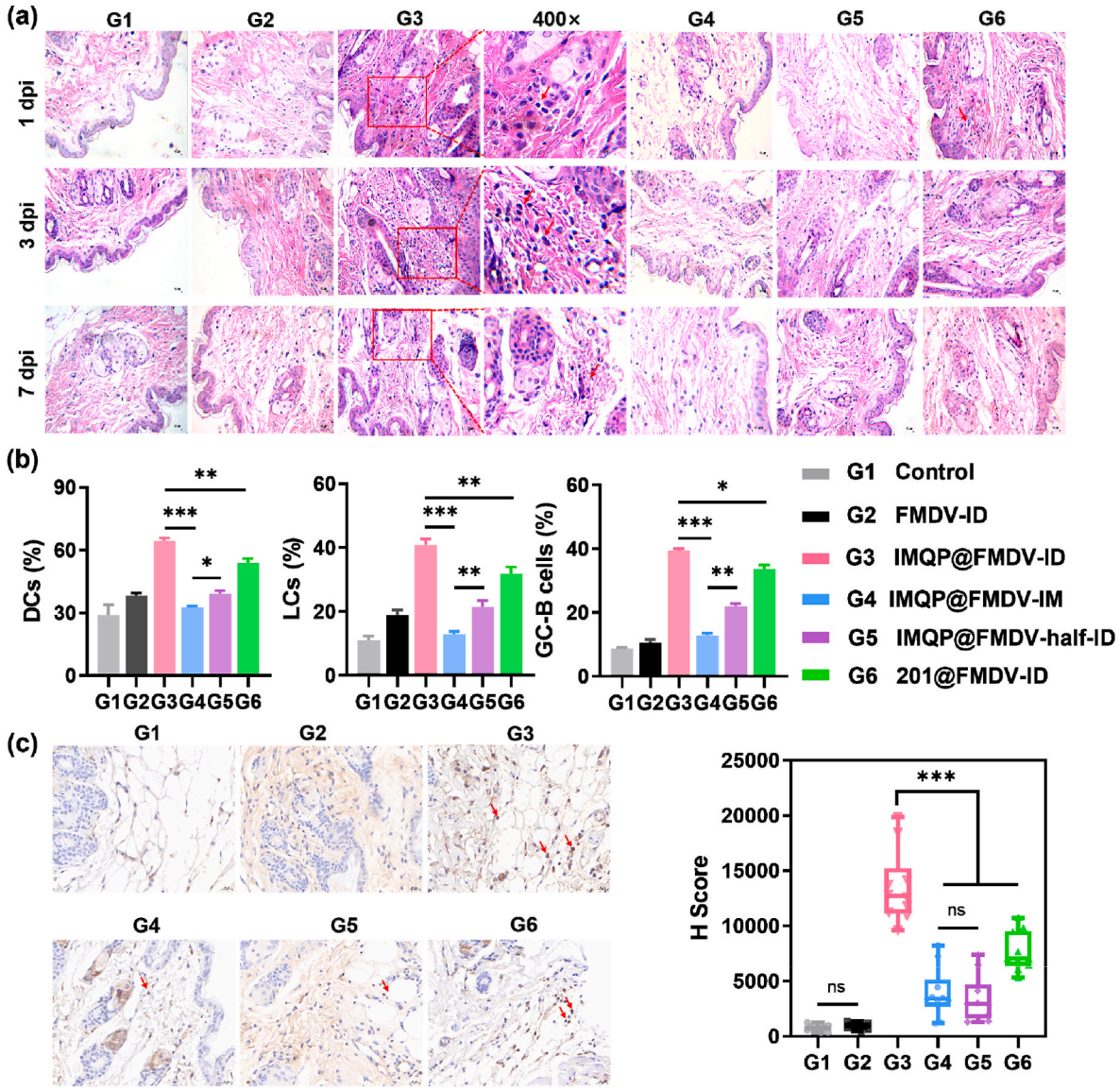

Fig. 3. APCs activation in skin tissue from 1 to 7 days after immunization in mice. (a) H&E staining of the skin at injection site in 1, 3, 7 dpi. Scale Bar: 50 μm. (b) The activation percentage of DCs, LCs and GC-B cells after 1 dpi by FACS. (c) IHC staining of skin after 7 dpi. Scale Bar: 20 μm. Results were expressed as means ± SD, n = 3, (*$P < 0.05$, **$P < 0.01$, ***$P < 0.001$, and ns = no significant differences between groups).

elicit local immunity and further continuously stimulate the IgG antibody expression.

Continuous antigen presentation and effective activation of dendritic cells (DCs) in lymph nodes (LNs) were beneficial for the formation and maintenance of T follicular helper (Tfh) cells in the germinal centers (GCs) [21]. Researches [22,23] indicated that B cells experienced somatic hypermutation in the GCs of secondary lymphoid organs and produced activating germinal center B (GC-B) cells with high affinity, which subsequently developed into memory B cells and long-lived plasma cells to produce high-quality antibodies to achieve the vaccine effect [18–20]. The fluorescence activated cell sorting (FACS) results (Fig. 3b and Fig. S3) indicated that numbers of DCs ($P < 0.001$), LCs ($P < 0.001$) and GC-B cells ($P < 0.001$) increased significantly in skin after 1 dpi with I.D. route. The activation ability of APCs by IMQP was stronger than that of commercial ISA201 with I.D. route ($P < 0.05$ or $P < 0.01$). Moreover, when the antigen dose was reduced by half for I.D. injection (IMQP@FMDV-half-ID), DCs ($P < 0.05$), LCs ($P < 0.01$) and GC-B cells ($P < 0.01$) were still significantly enhancement comparing with IMQP@FMDV-IM group. These data were consistent with the skin H&E results (Fig. 3a), indicating that IMQP was more suitable for I.D. immunization to activate APCs.

Then, we utilized the immunohistochemistry (IHC) to analyze the positive proportion of LCs in 7 dpi (Fig. 3c). There was no significant difference between the F-ID group and the control ($P > 0.05$). IMQP found that I.D. immunization could greatly induce the increase of LCs level, which was 4.3 times that of I.M. injection ($P < 0.001$). It was interesting that there was no significant difference between the expression level of LCs between the half-dose of I.D. immunization pathway and the full dose of muscle immunization ($P > 0.05$). Meanwhile, the LCs in IMQP@FMDV-ID group were increased by 14.7-fold, 6.73-fold, 5.78-fold and 1.8-fold higher compared with FMDV-ID, IMQP@FMDV-IM, IMQP@FMDV-half-ID and 201@FMDV-ID groups, respectively. In conclusion, IMQP-adjuvanted combined with intradermal immunity could recruit more APCs and thereby enhanced the immune response.

2.3. Intradermal delivery of IMQP elicits strong immunity responses

Skin-based vaccinations had shown to be an effective immunization route for a variety of pathogens like influenza, monkeypox and hepatitis B virus [24]. The level of anti-FMDV IgG was proposed to be directly correlated with vaccination potency. In order to estimate the immunity enhancement of IMQP adjuvant with I.D. injection, we used PBS as the negative control group and the inactivated FMDV vaccine adjuvanted with the commercially adjuvant ISA201 as the positive control group. As shown in Fig. 4a–c, the group of mice injected with FMDV did not exhibit antibody response, which was no significantly different from the control group. According to Fig. 4a and b, as expected, the

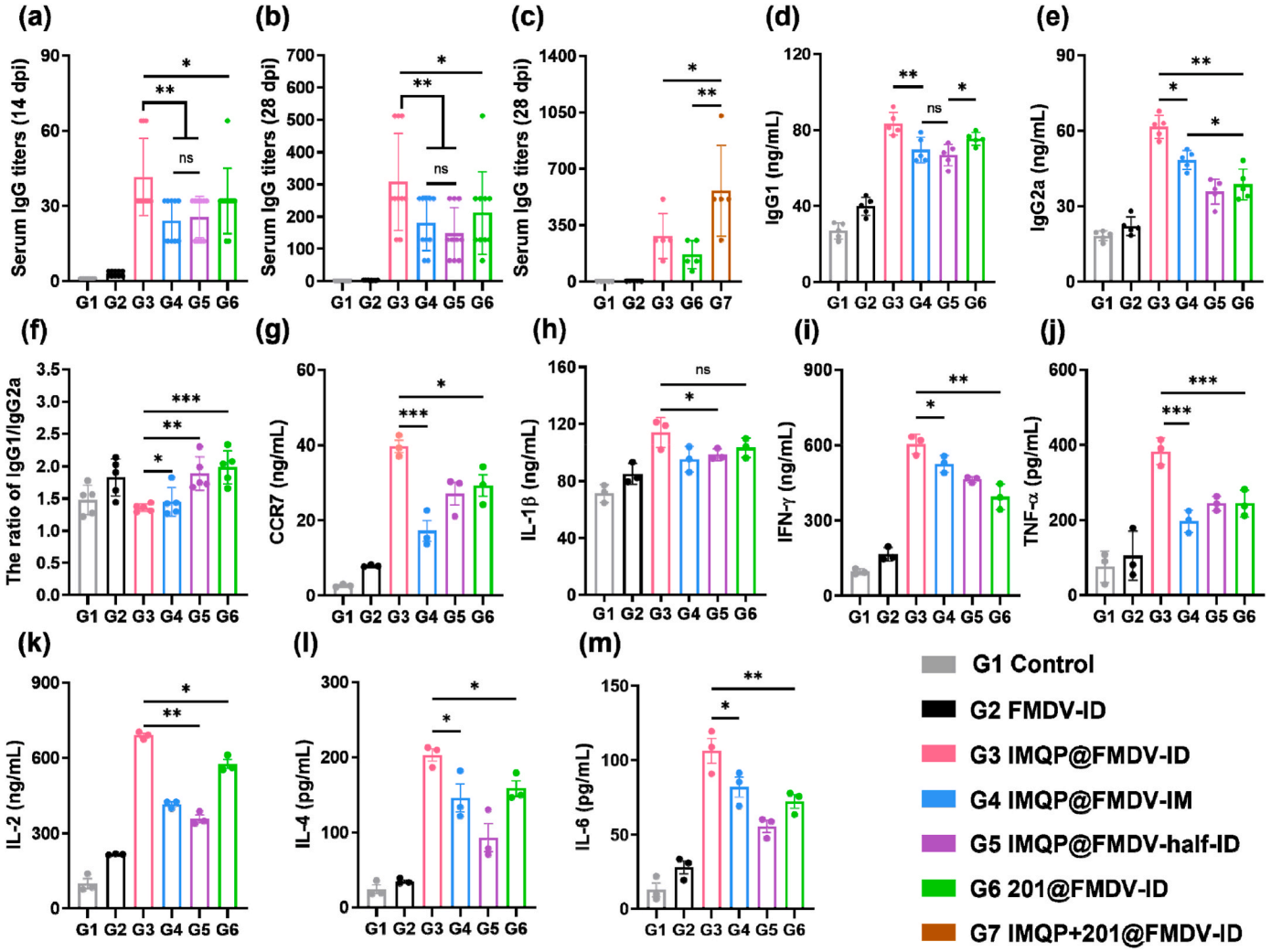

Fig. 4. Expression of specific antibodies and cytokines. The mice were immunized by intradermal on day 1 and strengthened-immune on day 14. The FMDV-specific antibody level of IgG (a–c), IgG1 (d), IgG2a (f), the ratio of IgG1/IgG2a, and cytokines (g–m) in serum were detected on day 14 or 28 after the first immunization. Results were expressed as means ± SD, n ≥ 3, (*$P < 0.05$, **$P < 0.01$, ***$P < 0.001$, and ns = no significant differences between groups).

specific-FMDV IgG was increased in all mice immunized with adjuvants at 14 dpi and 28 dpi, compared to mice immunized with the FMDV alone. The levels of IgG that received IMQP@FMDV-ID immune had dramatically exceeded than that of immunizing with 201@FMDV-ID ($P < 0.05$), IMQP@FMDV-IM ($P < 0.01$) and IMQP@FMDV-half-ID ($P < 0.01$) groups within 28 days. Interestingly, after halving the dosage, the level of the IgG antigen produced by I.D. immunization only slightly decreased comparing with I.M. injection at the full dose without significant statically differences t ($P > 0.05$). Notably, seeing from Fig. 4c, co-injection of IMQP and ISA201 formulation group elicited the highest level of anti-FMDV antibody titer (approximately 3.2-fold of 201@FMDV-ID group, $P < 0.01$ and nearly 1.6-fold of IMQP@FMDV-ID group, $P < 0.05$) in 28 dpi. The results demonstrated that combining IMQP and ISA201 could synergistically enhanced the immune potency.

Basophils play an important role in the development of type 2 immunity [25,26]. So, we examined the blood routine of mice at days 7 and 14 after immunization (Figs. S4 and S5). As illustrated in Fig. S4, after 7 dpi, the numbers of basophils in IMQP@FMDV-ID group were above the normal ranges, and significantly higher than that in other immune groups. These findings were consistent with the reported in the literature [27,28], suggesting that IMQP@FMDV-ID group could activate basophils to promote Th2 polarization to secrete IL-4 and IL-6, as well as trigger B cells survival, activation, differentiation and antibody production. Continuous observation showed that the basophilic returned to the normal range after 14 dpi (Fig. S5). These data proved that IMQP@FMDV nano-vaccine combining with I.D. immunization could induce an immune response in the short term by stimulating the inflammatory response, but did not affect animal health.

To further identify the nature of immunological response elicited by IMQP *via* I.D. route, the pattern of IgG antibody subclasses was evaluated using the Th1 and Th2 immune responses as indicators (Fig. 4d and e). Generally, IgG1 was commonly associated with the secretion of Th2 cells to induce humoral immune response [29]. However, the production of IgG2a tended to cell-mediated immune response, suggesting the Th1 cells elevation. Our findings showed that I.D. immunization using FMDV alone failed to significantly increased IgG1 or IgG2a antibody levels. Interestingly, when FMDV paired with IMQP to formulate an I.D. vaccination, the IMQP@FMDV nano-vaccine significantly increased the concentration of IgG1 antibody ($P < 0.01$) in comparison to I.M. immunization. The results demonstrated that IMQP with I.D. route could enhance Th2-type response also, which attributed to the abundance of APCs in the skin to better recruit, transport antigen and activate innate immunity. These outcomes were in line with the pattern shown in the H&E and IHC analyses (Fig. 3a and c), suggesting that IMQP was able to attract more LCs and inflammatory cells. In addition, a half dose antigen of vaccine (IMQP@FMDV-half-ID) still produced IgG1 antibody, which was not significant different from that of the IMQP@FMDV-IM ($P > 0.05$), but weaker than that of 201@FMDV-ID group ($P < 0.05$).

Furthermore, compared with 201@FMDV-ID group, the level of IgG2a was significantly increased after the addition of IMQP ($P < 0.01$), suggesting that IMQP as a TLR7 agonist induced Th1 immune response. When given the same dosage of the IMQP@FMDV vaccination, the I.D. route generated more IgG2a than the I.M. route ($P < 0.05$). Half-dose antigen of IMQP@FMDV nano-vaccine with I.D. immunization produced IgG2a slightly less than that of the I.M. immunization effect at the full dose, but overall showed no significant difference ($P > 0.05$). Also, in Fig. 4f, the ratio of IgG1/IgG2a in IMQP@FMDV-ID group was the lowest in the experimental groups. So, we could assume that IMQP acted as an adjuvant to enhance the cellular immune bias also. Overall, it was speculated that IMQP@FMDV-ID group exerted a strong Th1 and Th2 immune effect, which could be attributed to the following reasons: (1) IMQP, as a TLR7 agonist, could activate the cellular immune response and act as an antiviral effect; (2) the skin had so vast number of APCs that constantly were attracted and activated in situ; (3) small size of IMQP@FMDV LNPs are easy to be ingested by cells, thus increasing the intake of antigens. In addition, due to the weak alkaline of 1, 5 -position nitrogen atom in IMQP molecule, IMQP could be partly protonated in acidic lysosome and produced the phenomenon of "lysosome escape".

DCs interacted with T cells through antigen presentation action to regulate vaccine immune response, and promoted the production of IgG, IgG1 and IgG2a. During this process, Th1 and Th2 cells secreted different cytokines, in which IL-2 and IFN-γ were secreted by Th1 cells, and IL-4 was secreted by Th2 cells [30]. Moreover, CCR7 activated, participated and transported lymphocytes in LNs and spleen, and stimulated the DCs maturation [31]. Upon maturation of DCs would be also secreted pro-inflammatory cytokines like TNF-α, IL-1β and IL-6 thus regulating T cells. Representative relevant immune cytokines in peripheral blood serum also be tested. Serum levels of key immunoregulatory cytokines were monitored on 28 dpi (Fig. 4g–m). Compared with 201@FMDV-ID, immunization with IMQP@FMDV -ID could remarkably improve the levels of CCR7 ($P < 0.01$), IFN-γ ($P < 0.01$), TNF-α ($P < 0.001$), IL-2 ($P < 0.01$), IL-4 ($P < 0.05$), and IL-6 ($P < 0.01$) in serum, but did not result in a significant enhancing level of IL-1β ($P > 0.05$) in serum. So, we could presume that IMQP evoked stronger both Th1 and Th2 immune response. Furthermore, compared with immunization by I. M. route, IMQP@FMDV with I.D vaccination produced higher expressions of CCR7 ($P < 0.001$), IL-1β ($P > 0.05$), IFN-γ ($P < 0.05$), TNF-α ($P < 0.001$), IL-2 ($P < 0.01$), IL-4 ($P < 0.05$) and IL-6 ($P < 0.05$). On the whole, the IMQP@FMDV vaccine formulation with I.D. injection evoked stronger levels of both Th1 and Th2 cytokine secretion, indicating stronger immune responses [32].

2.4. Activation of T cells in draining lymph nodes (DLNs) and spleen

As one of the key locations for producing lymphocytes and the IgG antibodies in the body, LNs were the site of APCs migration and antigen-presenting function [33]. APCs could activate T lymphocytes to proliferate into helper T cells ($CD4^+$ T cells) and cytotoxic T lymphocytes ($CD8^+$ T cells, CTLs), and then triggered the ensuring immune response. Of note, the ratio of $CD4^+$ T cells to $CD8^+$ T cells was presently thought to be a crucial parameter for evaluating cellular immune responses. Also, CD3, as a specific marker of T lymphocytes, represented the degree of activation of T cells. After immunization, T cells in the drainage lymph nodes(DLNs)near the injection site were activated in 1 dpi, and the percentages of $CD3^+$ T cells in the IMQP@FMDV-ID, IMQP@FMDV-IM, IMQP@FMDV-half-ID and 201@FMDV-ID groups were about 62.6 %, 48.1 %, 46.1 % and 31.2 % respectively (Fig. S6). A massive amount of $CD3^+CD4^+$ T cells stimulated the mice's humoral and cellular immunological responses by upregulating their systemic immune response, while the high amount of $CD3^+CD8^+$ T cells could directly mediate the antigen specific cellular immune response. Further analyzing the extent of $CD4^+$ and $CD8^+$ activation, we found that the IMQP@FMDV vaccine with I.D. immunization had the highest proportion of $CD3^+CD4^+$ and $CD3^+CD8^+$, which were at 43.9 % and 18.4 %, respectively (Fig. 5a–c). There was no significant difference between IMQP@FMDV-half-ID and IMQP@FMDV-IM in $CD3^+CD4^+$ ratio ($P > 0.05$), but the percentage of $CD3^+CD8^+$ ($P < 0.05$) in IMQP@FMDV-IM group was higher than that of IMQP@FMDV-half-ID group. Compared with IMQP@FMDV-IM and 201@FMDV-ID groups, the $CD4^+/CD8^+$ ratio of the IMQP@FMDV-ID group was slightly lower than the IMQP@FMDV-IM group with no significant difference ($P > 0.05$), but significantly lower than the 201@FMDV group ($P < 0.05$) (Fig. 5d). The results suggested that IMQP, like other TLR7 agonists, was more likely to activate DCs [34], elicited a Th1 immune response and improved the generation of $CD8^+$ T cells, thus could be exploited to enhance the efficacy of antiviral vaccination.

In addition, the spleen, as an important immune organism, plays an vital role in anti-inflection because it possesses amounts of T and B cells [35]. The proliferation of splenic lymphocytes was positively correlated with the level of cellular immune response, which reflected the body's immune response [36]. After 28 dpi, the spleen lymphocytes were stimulated by FMDV and LPS *in vitro* respectively (Fig. 5e). After LPS

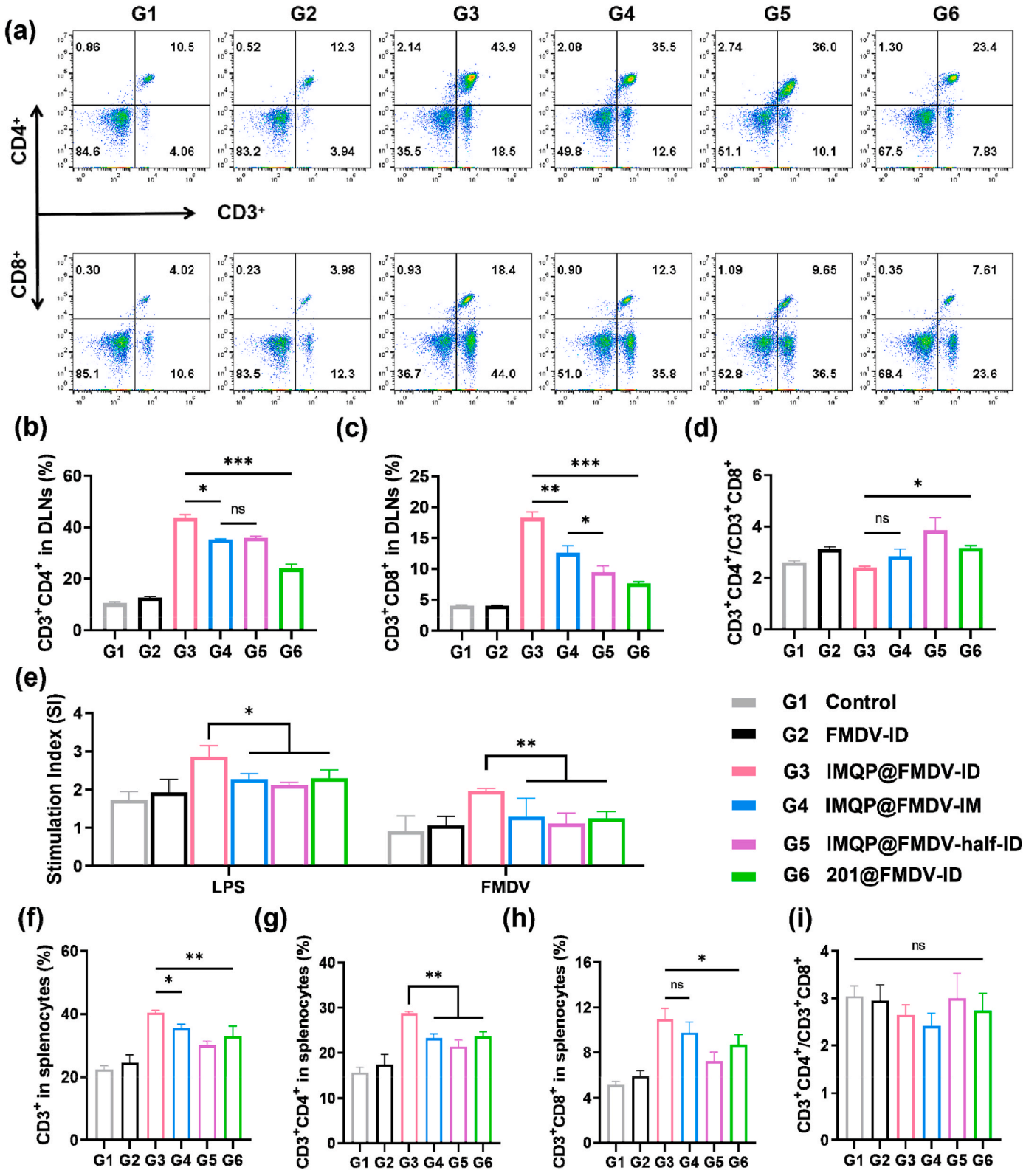

Fig. 5. IMQP promotes T cells activation in DLNs and spleen. (a–c) Proportion of differentiation into $CD4^+$ and $CD8^+$ from $CD3^+$ T cells activation in DLNs, and (d) The ratio of $CD4^+/CD8^+$ T cells activation. (e) Proliferative responses of splenocytes responding to LPS and FMDV *ex vivo*. (f) The percentage of activated $CD3^+$ T cells, and (g, h) proportion of differentiation into $CD4^+$ and $CD8^+$ from $CD3^+$ T cells activation in splenocytes, and (I) The ratio of $CD4^+/CD8^+$ T cells activation. Results were presented as mean ± SD, n = 3, (*$P < 0.05$, **$P < 0.01$, ***$P < 0.001$, and ns = no significant differences between groups).

stimulation, the SI of the control group, FMDV-ID, IMQP@FMDV-ID, IMQP@FMDV-IM, IMQP@FMDV-half-ID and 201@FMDV-ID were 1.72, 1.92, 2.86, 2.30, 2.11 and 2.28, respectively. After FMDV stimulation, the stimulation index (SI) was 0.91, 1.06, 1.96, 1.24, 1.11 and 1.29, respectively. These findings confirmed that IMQP combining with I.D. immunization could obtained a better immune memory effect than those of other groups. This could help them produce specific immune responses quickly and potently when having an encounter with the same antigen. Similar to the DLNs results, the IMQP@FMDV-ID group had the largest proportion of $CD3^+$, $CD3^+CD4^+$ and $CD3^+CD8^+$ T cells in splenocytes compared to 201@FMDV-ID and IMQP@FMDV-IM groups (Fig. 5f–h and Fig. S7). Notably, the CD4/CD8 ratio of IMQP@FMDV-ID group was not different from that of other groups ($P > 0.05$), indicating that IMQP could simultaneously stimulate humoral immunity and cellular dual immunity and maintain the balance of Th1/2 antibody response. Hence, the results *in vivo* suggested that the IMQP with I.D. route could induce an effective Th1 and Th2 immune response *via* DC maturation and infiltration of T cells, which leads to practical anti-virus effects.

2.5. IMQP@FMDV nano-vaccine promotes antigen uptake and activation of BMDCs

DCs are critical for inducing vaccine-mediated immune responses due to their unique ability to activate naive T cells. Thus, the good delivery ability of antigen and uptake by DCs are prerequisite for antigen

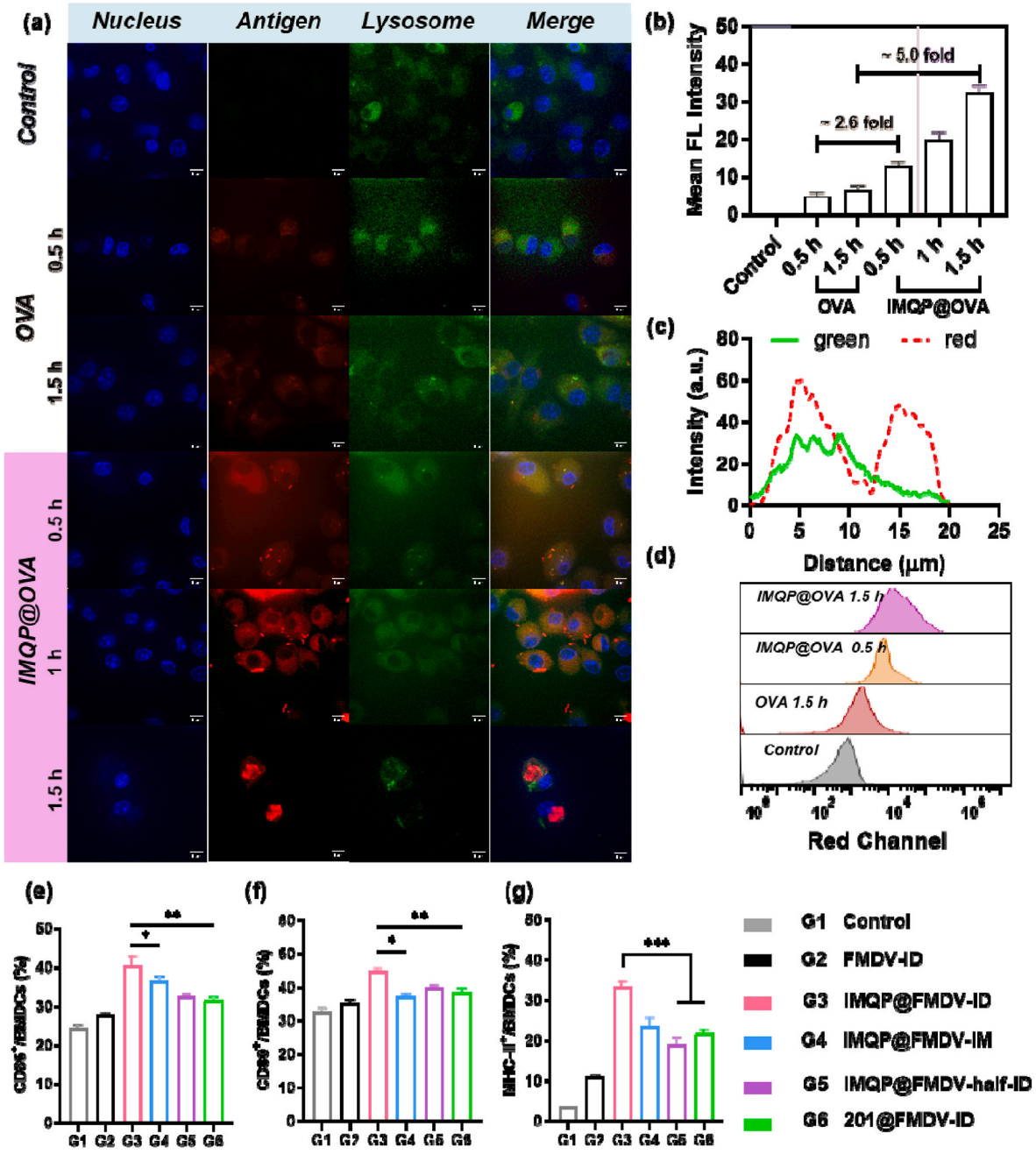

Fig. 6. Effects of IMQP nano-adjuvant on BMDCs uptake and activation. (a) The CLSM images of IMQP@OVA LNPs to cellular uptake by BMDCs within 0.5–1.5 h. (b) Mean red fluorescence intensity corresponding to control, OVA-Rh B and IMQP@OVA-Rh B in different time. (c) The colocalization correlation image of the intensities of OVA-Rh B and Lyso-Tracker Green and (e–g) Expression of $CD80^+$, $CD86^+$ and MHC-II^+ on BMDCs in 7 dpi by flow cytometry plots. Scale Bar: 5 μm. Results were presented as mean ± SD, n = 3, (*$P < 0.05$, **$P < 0.01$, ***$P < 0.001$, and ns = no significant differences between groups).

presentation and stimulation of immune response. To further evaluate the uptake efficiency of antigens, the OVA-Rh B was performed to trace the uptake efficiency of antigens. After co-incubation BMDCs with free OVA-Rh B or IMQP@OVA-Rh B NPs for 0.5–1.5 h, the antigen location inside the BMDCs is visualized by CLSM. The result showed only little antigen is taken up by the DCs of free OVA-Rh B group, while IMQP could deliver more antigen for cellular uptake (Fig. 6a). After 0.5 h of incubation, there was more than a two-fold difference in red fluorescence intensity between OVA-Rh B alone and IMQP@OVA-Rh B NPs. With prolonging phagocytosis, after 1.5 h, the fluorescence intensity of IMQP@OVA-Rh B increased by nearly 5 times compared with OVA-Rh B alone (Fig. 6b). Also, with the extension of co-incubation time, red and green fluorescence were separated, at the same time, after 1.5 h, OVA (red) and lysosome (green) fluorescence colocalization curves clearly did not overlap (Fig. 6c), indicating that OVA escaped from the lysosome and was re-released in the cytoplasm. Lysosomal escape is a critical mechanism to release antigens into the cytosol-an indispensable process for effective cross-presentation by DCs [37].Due to the weak alkaline nature of the 3-position and 5-position nitrogen atoms in IMQP molecules [38], we speculate that the IMQP undergoes part protonation in the acidic environment of lysosomes (pH 4.5–5.5), which promotes the lysosomal escape to release antigens into the cytoplasm. The FACS findings (Fig. 6d) also confirmed that IMQP can carry more antigens into cells quickly.

Also, high levels of the co-stimulators CD80 and CD86 were expressed on mature dendritic cells (mDCs) and provided essential signal for presenting antigen and activating naive T cells [39]. BMDCs were usually quiescent *in vivo* and changed from quiescent to activation in response to antigen or related cytokine stimulation. After engulfing the antigens coming from the injection site, BMDCs migrated to nearby LNs through the lymphatic system to interact with T cells, where they differentiate into mature BMDCs. Meanwhile, the activation process of BMDCs was accompanied by high expression and secretion of surface markers, including MHC-II, CD80 and CD86. MHC-II molecules presented proteins for T cells to perform humoral response. Consequently, to gain insights into the role of IMQP as an adjuvant, we measured the expression of BMDCs surface co-stimulatory molecules and estimated the activation and maturation of BMDCs (Fig. 6e–g and S8). The expressions of MHC-II, CD80 and CD86 in the 201@FMDV-ID group were not significantly different from that in the IMQP@FMDV-IM group, while IMQP@FMDV-ID group significantly up-regulated the expression of CD80 ($P < 0.01$), CD86 ($P < 0.01$) and MHC-II ($P < 0.001$). Compared to the IMQP@FMDV-IM group, the expression of MHC-II had not be improved, but expression of CD80 and CD86 were significantly different change ($P < 0.05$). IMQP, as a small-molecule immune activator, activated BMDCs *via* the TLR7-dependent pathway, and bond with relevant T cell receptor (TCR) through $CD80^+$, $CD86^+$ and $MHC\text{-}II^+$, as well as enhanced pro-inflammatory cytokine secretion to regulate the differentiation of T cells. Our results verified that IMQP could promote the activation and maturation of DCs, could be used as a potential intradermal vaccine adjuvant to deliver antigens, and induce more effective immune responses.

2.6. Biosafety study of IMQP@FMDV vaccine in vivo

The IMQP@FMDV vaccine was formulated by re-precipitation strategy mixing IMQP with inactivated FMDV. After immunization with different administration routes, the clinical features of these immune mice were continuously observed. During the vaccination period, we weighed the mice weekly and found that the weight of the mice in each experimental group grew with time, and no differed considerably with the blank group. Meanwhile, the IMQP@FMDV vaccine *via* the I.D. or I.M. route cause no clear effect on the body weight ($P > 0.05$) and all mice grew as expected (Fig. S9a).

After 28 dpi, the indices of ALT, ALP, AST, LDH and BUN were detected by blood biochemical analysis, which judged the functions of liver, kidney and heart were normal or not. As shown in Figs. S9b–f, compared with control group, there was no apparent change ($P > 0.05$) in the indices of ALT, AST, ALP, LDH, and BUN using the IMQP@FMDV vaccine with multiple injection routes, which were still within the expected ranges and lacked unwelcome ups and downs.

2.7. Induction of TLR7 signal pathway

Molecular docking was a process identified by simulating ligand and receptor in spatial shape matching and energy matching, i.e., the process of "induced matching". In order to identify TLR7 agonistic activity of IMQP, we used molecular docking technique to simulate the docking of IMQP with mouse TLR7 receptor. As shown in Fig. S10, IMQP without self-immolating spacers quickly entered the hydrophobic cavity of TLR7 receptor and form a powerful intermolecular force with the surrounding amino acid residues such as Phe485, Pro482 and Lys679. Hence, the theory results also successfully verified that the IMQP stimulated the TLR7 pathway and boosted the immune potency.

To further investigated whether TLR7 signal pathway was activated by IMQP treatment, BMDCs were stimulated with IMQP for 4 h and the expressions of key proteins involved in the pathway were examined with Western-Bolt. As illustrated in Fig. S11, compared with un-treated BMDCs, both IMQ and IMQP could induced the high protein expression of TLR7 ($P < 0.001$) and MyD88 ($P < 0.001$), which demonstrated IMQP, like IMQ, acted as a TLR7 agonist and activated MyD88 signal transduction pathway. Interestingly, IMQP showed stronger protein expression of TLR7 ($P < 0.001$) than parent IMQ group, which was benefiting from slow-release ability of IMQP to continuously stimulate immune response. Thus, IMQP could enhance the antiviral inflection ability of body. The mitogen-activated protein kinase (MAPK) pathway has been closely associated with many cellular stresses, including inflammatory responses. Further, NF-kB is considered to be an important transcription factor involved in mediating inflammatory processes. Actually, transcription factors of NF-κB and MAPK were the essential role of TLR7 signal pathway. Therefore, we examined the expressions of key proteins involved in the two pathways. In addition, IMQP also induced the phosphorylation of ERK, p38 and p65. Hence, the data suggested that the MyD88 adaptor protein for TLR7 receptor and these key proteins triggering MAPK and NF-κB pathways were activated by IMQP. These results could be explained because TLR7 boosted high level expressions of pro-inflammatory cytokines such as IL-1β, IL-6 and TNF-α, promoted migrating DCs to recruit lymphocyte, and activated the immune response directly.

A better understanding of immunization mechanism for preventing virus infection is urgently needed to improve vaccine efficacy. Therefore, we employed RNA-seq to analyze the immunization mechanism of IMQP. DESeq software (Version 1.18.0) was used for differential expression analysis to identify candidate genes regulated by IMQP treatment. From the cluster analysis of DEGs, there was significant genetic difference among control and IMQP groups and the gene repeatability was well (Fig. S12). The Venn diagram showed significant differences between the major transcripts in the IMQP and control groups (Fig. 7a). A total of approximately 153 DEGs were distinguished between the control group and IMQP groups in the volcano plot, of which 85 up-regulated and 68 down-regulated ($|\log_2 FoldChange| > 1$ and P-value <0.05) (Fig. 7b). Subsequently, the biological characteristics of the potential targets of IMQP were evaluated by GO and KEGG analyses. GO analysis (Fig. 7c) showed that the DEGs were mainly enriched in immune-related pathways, including immune response, T cells receptor signal pathway, signal transduction and regulation of lymphocyte activation, indicating that IMQP induced powerful and comprehensive immunity *via* induced cytokines and chemokines. Furthermore, the pathway-related gene expression from the heatmap of DEGs, such as TLR7, CCL3, CXCL10, was up-regulated with IMQP groups compared with control group, indicating that IMQP could exert humoral and cellular immune responses by modulating related the regulating

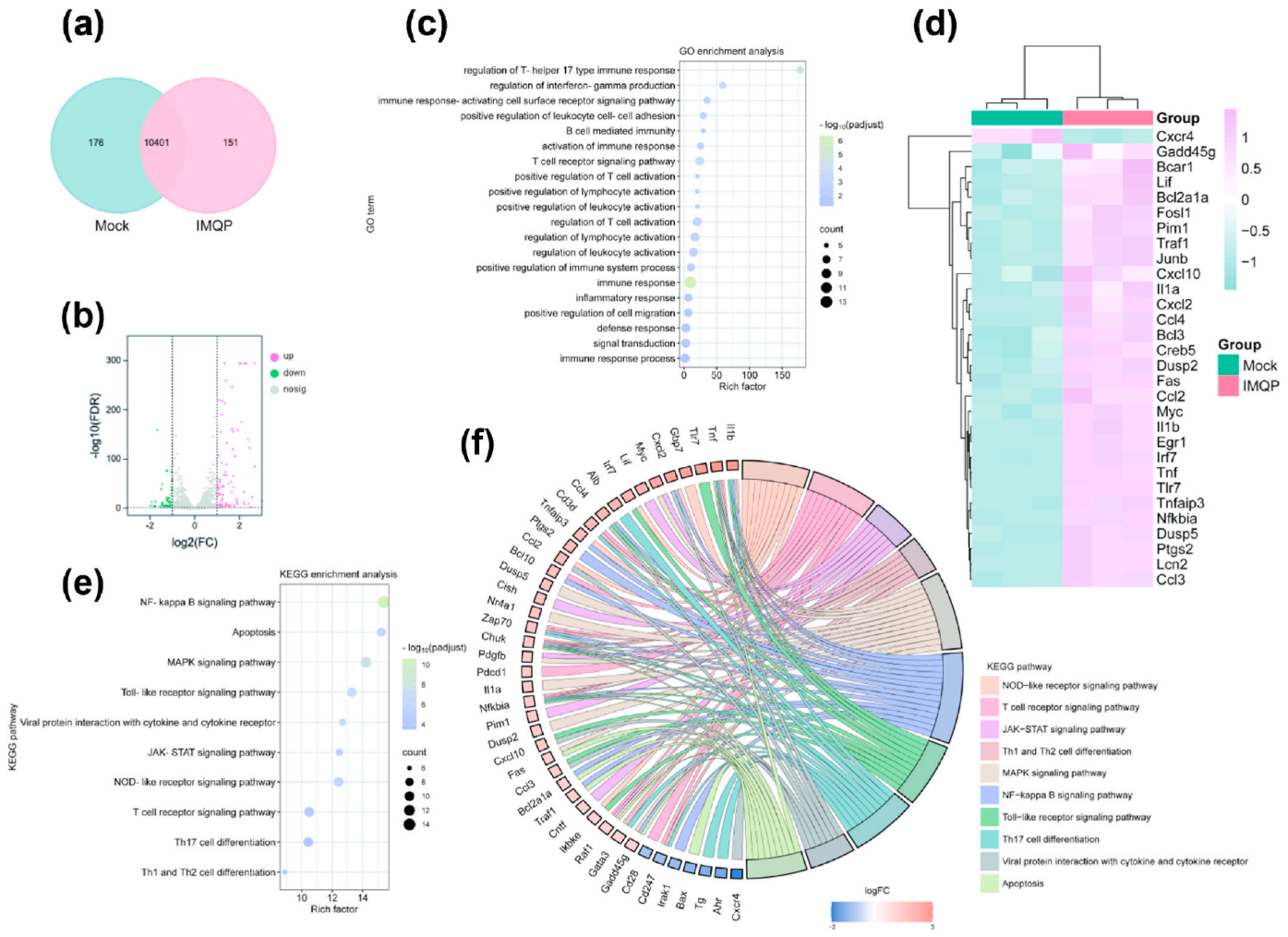

Fig. 7. RNA-seq analysis of BMDCs treated with IMQP for 4 h. (a) Venn diagram of the differentially expressed genes in Mock and IMQP groups. (b) Volcano plot of fold changes of the genes identified at $q < 0.05$. (c) GO enrichment analysis showing the main 20 immune-related pathways in which the differentially expressed genes of IMQP versus Mock were enriched. (d) Heat map of immune-related gene expression in IMQP treated BMDCs. (e) Categorization of the differentially expressed genes of immune in IMQP treated BMDCs, as observed by KEGG enrichment analysis. (f) Enriched chord diagram of the differentially expressed genes based on KEGG enrichment analysis.

different proinflammatory cytokines and chemokine genes (Fig. 7d). In the same time, KEGG enrichment analysis results (Fig. 7e and f) demonstrated that IMQP could promote the related signaling pathways including TLR, NF-κB and MAPK, Th17 cell differentiation and so on. Furthermore, the RNA-seq analysis results also suggested that IMQP could activate the TLR7 pathways and dramatically up-regulate immune-related gene expression, which were almost consistent with the parent IMQ.

As is known to all, amide bond is prone to hydrolysis *in vivo* and *in vitro*. In view of the above, we speculated that the expression of TLR7 signaling pathway for the adjuvant IMQP comes from IMQ, which come from the product of hydrolysis of IMQP. In order to check the hydrolysis profile of IMQP, we used HPLC to trace hydrolysis reaction products of IMQP in DMSO/PBS ($v/v = 9{:}1$, pH = 5.5) at 37 °C (Figs. S13 and S14). The retention time of IMQP, IMQ and solvent DMSO were 3.34, 1.93 and 1.58 min, respectively. However, when the IMQP kept in DMSO/PBS at 37 °C for 72 h, we could observe a new obvious peak at about 1.89 min appeared, which suggested that IMQP underwent a hydrolysis reaction to generate IMQ. Moreover, we could still see the peak of after 72 h, demonstrating IMQP slow hydrolyzed and sustained long-term release of IMQ.

In addition, we randomly selected 10 DEGs for RT-qPCR validation. The results manifested that mRNA level of CXCR4 obviously down-regulated ($P < 0.01$), however, the mRNA levels of TLR7 ($P < 0.01$), IL-1α ($P < 0.01$), IL-1β ($P < 0.001$), TNF ($P < 0.001$), CCL2 ($P < 0.001$), CCL3 ($P < 0.05$), CCL4 ($P < 0.001$), CXCL2 ($P < 0.001$) and CXCL10 ($P < 0.001$) significantly upregulated. Those data were consistent with the RNA-seq results (Fig. S15). Taken together, the above results verified the conceivable mechanism by which exposure to IMQP activate TLR7/MyD88/NF-κB and MAPK signal pathways, and thereby stimulate the humoral and cellular dual immune response of the organism.

3. Conclusion

In summary, we successfully designed a lipidation TLR7 agonist IMQP as FMDV-based nano-adjuvant to induce both Th1- and 2-type immune response. The IMQP serves not only as a structural component of LNPs to enhance FMDV vaccine delivery, but also as a functional TLR7 moiety to target lysosome membrane of immune cells and to increase the adjuvanticity of the LNPs. Further study unveiled that IMQP@FMDV accompanying with I.D. inoculation could greatly improve the recruitment of immune cells at the injection site, obviously increased antigen presentation ability of APCs, and facilitated more lymphocyte differentiation, proliferation and maturation. IMQP improve the FMDV antigen uptake to DCs, and lysosomal escape was also confirmed by DCs co-localization. Moreover, the animal

experiments manifested that the IMQP@FMDV-ID group could safely and superiorly improve the expression of antibodies, along with a heightened differentiation of T lymphocytes. Significantly, the RNA-seq and Western-Bolt analysis revealed that the IMQP could activate the innate, and subsequent the adaptive immune responses *via* TLR7/MyD88/NF-κB and MAPK pathway through IMQ, arising from hydrolysis of IMQP *in vivo*. Our research showed that IMQP could be used as an intradermal adjuvant to enhance immune response, which provides a new idea for the synthesis of lipid- or water-soluble TLR7 adjuvants for the development and application of immunoadjuvants. Considering its excellent physicochemical properties, TLR7 antagonist activity, assembly into LNPs, and good biocompatibility, the IMQP may be used alone or in combination with other adjuvants to prepare other antiviral vaccines, such as pseudorabies virus, porcine circovirus, and so on.

4. Materials and methods

4.1. Chemicals and reagents

Analytical-grade chemicals and solvents were all utilized further purification. Palmitoyl chloride (97 %), methanol (AR, 99.5 %), ethanol (AR, 99.5 %), 4-dimethylaminopyridine (DMAP, AR, 99 %), ethyl acetate (EA, AR, 99.5 %) and dichloromethane (CH_2Cl_2, DCM, AR, 99.5 %) and Tween-20 were commercially obtained by Nanjing Reagent Co., Ltd. Imiquimod (IMQ, 99 %) was obtained from Macklin (Nanjing). Collagenase, hyaluronidase, fetal bovine serum (FBS), the cell culture media of RPMI-1640 and DMEM were purchased from Gibco-Thermo Fisher (USA). ISA206 and ISA201 were sourced from SEPPIC (France). Inactivate FMDV antigen (the concentration 146S is about 300 μg/mL) was provided by Jinyu bio-technology Co., Ltd. A Milli-Q Biocel ultrapure water system with a resistance of 18.2 MΩ cm was utilized to treat deionized (DI) water. Information for antibodies, kits and else reagents were supplemented in the Supporting Information.

4.2. Cell and animals

Bone-marrow-derived dendritic cells (BMDCs) were separated from bone marrow cells in mouse femurs and used GM-CSF (20 ng/mL) to differentiation for 7 days. The red blood cells (RBCs) were collected from SPF chicken and diluted in PBS. RAW264.7 cells (ATCC, USA) were obtained from our own lab. And, ICR mice (aged 4-week-old, female) were purchased from the Comparative Medicine Center of Yangzhou University.

4.3. Synthesis and characterization of IMQP

To a solution of imiquimod (240 mg, 1 mmol) and 4-dimethylaminopyridine (DMAP, 244 mg, 2 mmol) in 20 mL of anhydrous CH_2Cl_2, palmitoyl chloride (412 mg, 1.5 mmol) was added at ice-bath. After stirring for 1 h, the mixture was refluxed for 4 h (Fig. S16). The resulting solution was diluted with CH_2Cl_2 (15 mL), then washed with H_2O (3 × 15 mL) and dried over anhydrous Na_2SO_4. The solvent was removed using rotary evaporation to give crude product of IMQP. Purification by silica gel column chromatography (CH_2Cl_2: ethyl acetate = 3:1) afforded a white solids with a final yield of 87 % (416 mg). ^{1}H NMR (400 MHz, $CDCl_3$) δ8.76 (s, 1H), 8.11 (d, J = 7.9 Hz, 1H), 8.01 (dd, J = 8.2, 0.9 Hz, 1H), 7.83 (s, 1H), 7.67–7.60 (m, 1H), 7.55–7.45 (m, 1H), 4.34 (d, J = 7.4 Hz, 2H), 3.08 (s, 2H), 2.37 (dt, J = 13.6, 6.8 Hz, 1H), 1.83 (dd, J = 15.2, 7.7 Hz, 2H), 1.46 (dd, J = 15.2, 7.4 Hz, 2H), 1.34–1.19 (m, 22H), 1.05 (d, J = 6.6 Hz, 6H), 0.88 (t, J = 6.9 Hz, 3H). ^{13}C NMR (101 MHz, $CDCl_3$) δ 175.61, 146.30, 144.39, 143.86, 135.01, 134.94, 131.07, 127.61, 127.34, 120.01, 118.58, 55.18, 38.23, 31.89, 29.65, 29.62, 29.57, 29.43, 29.36, 29.32, 29.06, 28.91, 24.49, 22.65, 19.86, 14.05, 14.02. (Notes: Due to two carbon peaks are buried between 29.2 and 29.70, which could be seen by local enlarged view, the data are missing two carbon peaks. Seeing Figs. S17 and S18). HR-MS (ESI): *m/z* calcd for $C_{30}H_{47}N_4O^+$, $[M + H]^+$, 479.37444; found, 479.37256 (Fig. S19).

4.4. Synthesis and characterization of IMQP@FMDV, IMQP@OVA, and OVA-Rh B

The IMQP-based NPs were prepared by a re-precipitation strategy. Briefly, 12 mL 10 μg/mL FMDV antigen was slowly added into 2 mL DMF solution of IMQP (500 μg/mL) with stirring continuously (300 rpm) for 30 min at room temperature. After centrifuging, washing and freeze-drying, white IMQP@FMDV nano-vaccine with sticky feeling was obtained. In the same method, IMQP@OVA or IMQP@OVA-Rh B LNPs were fabricated. As a control, 10 mg of IMQP powers was dissolved in 5 mL of DMF to prepare solution A and 2 mg of OVA or OVA-RhB was dissolved in 20 mL of DI water to prepare solution B. Then, slowly added solution B into solution A with stirring (300 rpm) at room temperature to prepare LNPs.

The traditional approach was used to obtain the red fluorescence label OVA protein. Firstly, 5 mg Rhodamine B isothiocyanate was added into 2 mL DMSO to prepare a 2.5 mg/mL solution A. And dissolving 100 mg of OVA in 20 mL of 0.2 M $NaHCO_3/Na_2CO_3$ buffer (pH = 9.5) prepared a 5 mg/mL solution B. After mixing solution A and solution B at 4 °C for 24 h with stirring of 100 rmp; the solution was dialyzed for 48 h and freeze-dried to obtain OVA-RhB.

4.5. Histological and immunohistochemical (IHC) examination

Histological examination was performed for assessment of the toxicity of IMQP *in vivo*. In briefly, IMQP with 200 μg/mL or 1000 μg/mL were injected into mice through intraperitoneal (I.P.) pathway, respectively. After 7 days, the mice (three per group) were sacrificed. The primary organs (heart, liver, spleen, lung and kidney) were collected, preserved in 4 % paraformaldehyde (PFA) for 24 h, and then embedded in paraffin. Hematoxylin and eosin staining (H&E) were done in the sectioned tissues. Additionally, skin changes at the local injection site after I.D. injection of IMQP@FMDV vaccine in mice immunized at different times (day 1–7). IHC experiment was according to a professional experimental protocol, and the LCs were labeled with anti-Langerin antibody. The histological sections were photographed under an Olympus microscope (Olympus IX71, Tokyo, Japan).

4.6. Immunization, detection of anti-FMDV antibodies, and cytokines

Vaccine formulations of mice was injected by I.D. or I.M. in seven groups (n = 10) with a 100 μL dosage, including PBS as negative control (G1, Control), FMDV alone (G2, FMDV-ID), IMQP@FMDV nano-vaccine with I.D. vaccination (G3, IMQP@FMDV-ID) and I.M. vaccination (G4, IMQP@FMDV-ID), half dosage of IMQP@FMDV with I.D. vaccination (G5, IMQP@FMDV-half-ID), FMDV plus ISA201 (G6, ISA201@FMDV-ID) and IMQP@FMDV plus ISA201 (G7, IMQP+201@FMDV-ID). The FMDV was administrated at 1.2 μg per mouse of G2-G4, G6 and G7, and 0.6 μg per mouse of G5. The IMQP was administrated at 10 μg per mouse of G3, G4 and G5. Blood samples were obtained at 7, 14 or 28 days post-immunization (dpi). Sera were separated by centrifugation at 5000 rpm for 5 min and stored at −70 °C until antibody titers were tested.

FMDV-specific IgG and subtypes (IgG1, IgG2a), and cytokines (IL-1β, IL-2, IL-4, IL-6, IFN-γ, TNF-α and CCR-7) in serum of the immunized mice were detected by commercial ELISA kits on days 14 or 28 after according to instruction book. The absorbance was calculated at 450 nm by a microplate reader, and all samples were measured at least three.

4.7. Activation of APCs in injection local skin

Mice were sacrificed after vaccination. The skin coming from injection site at 1 dpi was digested using collagenase, hyaluronidase and DNase I, and then the APCs were collected by centrifugation. The obtained APCs were stained using fluorescence labeled antibodies,

including PE anti-mouse CD45R/B220, FITC anti-mouse CD11c, FITC anti-mouse GL7. At last, the stained cells were detected by flow cytometry (BD Accuri C6 Plus, USA) and analyzed with FlowJo software.

4.8. Cellular uptake by BMDCs

The antigen uptake efficiency of BMDCs was determined through confocal laser scanning microscopy (CLSM) and flow cytometry. The BMDCs were incubated in a confocal dish with OVA-Rh B (10 μg/mL) and IMQP@OVA-Rh B for different times (IMQP:50 μg/mL), washed using PBS, and added with 4 % PFA for 20 min to fix cells. Then, the cells were co-incubated with 200 μL of LysoTracker Green for 15 min and 50 μL of DAPI for 15 min in order to stain the lysosomes and nucleus. Finally, cells were used CLSM and flow cytometry to measure the OVA uptake efficiency.

4.9. RNA-seq analysis of BMDCs

The BMDCs were collected and submitted for investigation after mixing well with Fast Pure cell/tissue RNA isolation kit-box 2. Then, Biomaker Technologies Co., Ltd. then conducted RNA-seq analysis using a high-throughput sequencing technique. Fold Change $\geq$2 and FDR $<$0.01 were used as criteria for identifying differentially expressed genes (DEGs), and GO and KEGG analyses were then conducted to examine the pathways and functions of DEGs.

4.10. Hydrolysis of IMQP

In accordance with the literature [40] and previously described procedure [41], IMQP (0.15 mg) was dissolved 10 mL DMSO-PBS (v/v = 1:9, pH = 5.5) solution with stirring at 37 °C for 72 h, and the solution was taken immediately for the determination of initial concentrations of the HPLC and ESI-MS analytes.

The ZORBAX SB-C18 (4.6 mm × 150 mm, 5 μm) chromatographic column with a detection wavelength of 240 nm in SHIMADZU-LC-20AD was used for the HPLC analysis (The mobile phase: methanol, the column temperature: 40 °C, the flow velocity: 0.8 mL/min and the column pressure: 4.7 MPa).

4.11. Statistical analysis

Using Excel and GraphPad Prism 8.4.2 softwares to record and analyzed the experiments data, respectively. All results were presented as mean ± SD at least 3 independent studies. Statistical differences were compared using a one-way ANOVA test, which were considered to be significant using $^{*}P < 0.05$, $^{**}P < 0.01$ and $^{***}P < 0.001$.

CRediT authorship contribution statement

Wenzhu Yin: Writing – original draft, Methodology, Funding acquisition, Formal analysis, Conceptualization. **Zeyu Xu:** Validation, Formal analysis, Data curation. **Fang Ma:** Methodology, Funding acquisition. **Bihua Deng:** Supervision. **Yanhong Zhao:** Methodology. **Xiaoxin Zuo:** Formal analysis, Data curation. **Haiyan Wang:** Resources, Funding acquisition. **Yu Lu:** Writing – review & editing, Supervision, Resources, Funding acquisition.

Ethics approval and consent to participate

All animal experiment designs and protocols involving animal were approved by the Institutional Animal Care and Use of Committee (IACUC) at JAAS (No. SYXJK(Jiangsu) 2020-0024). The authors declare that all experiments involving animals were in compliance with relevant ethical regulations.

Declaration of competing interest

The authors declare that they have no known competing financial interests or personal relationships that could have appeared to influence the work reported in this paper.

Acknowledgments

This work was financially supported by the Natural Science Foundation of Jiangsu Province (No. BK20241181, BK20221431), State Key Laboratory of Analytical Chemistry for Life Science (No. SKLACLS2419), Jiangsu Association for Science and Technology Youth Science and Technology Talents Support Project (No. JSTJ-2024-114) and Jiangsu Agriculture Science and Technology Innovation Fund (JASTIF) (No. CX (2022)2018). Also, we thank Chunmei Wang from Central Laboratory in Jiangsu Agricultural Sciences for her technical support of confocal laser scanning microscopy.

Appendix A. Supplementary data

Supplementary data to this article can be found online at https://doi.org/10.1016/j.mtbio.2025.101567.

Data availability

Data will be made available on request.

References

[1] J. Arzt, M.W. Sanderson, C. Stenfeldt, Foot-and-Mouth disease, Vet Clin North Am Food Anim Pract 40 (2) (2024) 191–203.
[2] S. Mu, L. Chen, H. Dong, S. Li, Y. Zhang, S. Yin, Y. Tian, Y. Ding, S. Sun, S. Shang, H. Guo, Enhanced antigen-specific CD8 T cells contribute to early protection against FMDV through swine DC vaccination, J. Virol. 98 (2) (2024) e02002–e02023.
[3] L. Cheng, Z. Zhang, G. Li, F. Li, L. Wang, L. Zhang, S.M. Zurawski, G. Zurawski, Y. Levy, L. Su, Human innate responses and adjuvant activity of TLR ligands in vivo in mice reconstituted with a human immune system, Vaccine 35 (45) (2017) 6143–6153.
[4] E.C. Lavelle, C.P. McEntee, Vaccine adjuvants: tailoring innate recognition to send the right message, Immunity 57 (4) (2024) 772–789.
[5] Y. Wu, Z. Yang, K. Cheng, H. Bi, J. Chen, Small molecule-based immunomodulators for cancer therapy, Acta Pharm. Sin. B 12 (12) (2022) 4287–4308.
[6] S.-B. Yoon, H. Hong, H.-J. Lim, J.H. Choi, Y.P. Choi, S.W. Seo, H.W. Lee, C.H. Chae, W.-K. Park, H.Y. Kim, D. Jeong, T.Q. De, C.-S. Myung, H. Cho, A novel IRAK4/PIM1 inhibitor ameliorates rheumatoid arthritis and lymphoid malignancy by blocking the TLR/MYD88-mediated NF-κB pathway, Acta Pharm. Sin. B 13 (3) (2023) 1093–1109.
[7] P. Larson, T.A. Kucaba, Z. Xiong, M. Olin, T.S. Griffith, D.M. Ferguson, Design and synthesis of N1-modified imidazoquinoline agonists for selective activation of toll-like receptors 7 and 8, ACS Med. Chem. Lett. 8 (11) (2017) 1148–1152.
[8] U. Wille-Reece, B.J. Flynn, K. Loré, R.A. Koup, R.M. Kedl, J.J. Mattapallil, W. R. Weiss, M. Roederer, R.A. Seder, HIV Gag protein conjugated to a Toll-like receptor 7/8 agonist improves the magnitude and quality of Th1 and $CD8^{+}$ T cell responses in nonhuman primates, Proc. Natl. Acad. Sci. USA 102 (42) (2005) 15190–15194.
[9] J. Wang, H. Zope, M.A. Islam, J. Rice, S. Dodman, K. Lipert, Y. Chen, B.R. Zetter, J. Shi, Lipidation approaches potentiate adjuvant-pulsed immune surveillance: a design rationale for cancer nanovaccine, Front. Bioeng. Biotechnol. 8 (2020).
[10] X. Han, M.-G. Alameh, K. Butowska, J.J. Knox, K. Lundgreen, M. Ghattas, N. Gong, L. Xue, Y. Xu, M. Lavertu, P. Bates, J. Xu, G. Nie, Y. Zhong, D. Weissman, M. J. Mitchell, Adjuvant lipidoid-substituted lipid nanoparticles augment the immunogenicity of SARS-CoV-2 mRNA vaccines, Nat. Nanotechnol. 18 (9) (2023) 1105–1114.
[11] C.W. Hespen, X. Zhao, H.C. Hang, Membrane targeting enhances muramyl dipeptide binding to NOD2 and Arf6–GTPase in mammalian cells, Chem. Commun. 58 (46) (2022) 6598–6601.
[12] D. Smirnov, J.J. Schmidt, J.T. Capecchi, P.D. Wightman, Vaccine adjuvant activity of 3M-052: an imidazoquinoline designed for local activity without systemic cytokine induction, Vaccine 29 (33) (2011) 5434–5442.
[13] Z. Zhong, Y. Chen, K. Deswarte, H. Lauwers, E. De Lombaerde, X. Cui, S. Van Herck, T. Ye, M. Gontsarik, S. Lienenklaus, N.N. Sanders, B.N. Lambrecht, S. De Koker, B.G. De Geest, Lipid nanoparticle delivery alters the adjuvanticity of the TLR9 agonist CpG by innate immune activation in lymphoid tissue, Adv. Healthcare Mater. 12 (32) (2023) 2301687.
[14] Z. Liu, Q. Wang, Y. Feng, L. Zhao, N. Dong, Y. Zhang, T. Yin, H. He, X. Tang, J. Gou, L. Yang, The self-adjuvant heterocyclic lipid nanoparticles encapsulated with

vaccine and STAT3 siRNA boost cancer immunotherapy through DLN-targeted and STING pathway, Chem. Eng. J. 475 (2023) 146474.
[15] G. Du, M. Qin, X. Sun, Recent progress in application of nanovaccines for enhancing mucosal immune responses, Acta Pharm. Sin. B 13 (6) (2023) 2334–2345.
[16] S. Mao, S. Li, Y. Zhang, L. Long, J. Peng, Y. Cao, J.Z. Mao, X. Qi, Q. Xin, G. San, J. Ding, J. Jiang, X. Bai, Q. Wang, P. Xu, H. Xia, L. Lu, L. Xie, D. Kong, S. Zhu, W. Xu, A highly efficient needle-free-injection delivery system for mRNA-LNP vaccination against SARS-CoV-2, Nano Today 48 (2023) 101730.
[17] Y. Wu, S. Yu, I. de Lázaro, Advances in lipid nanoparticle mRNA therapeutics beyond COVID-19 vaccines, Nanoscale 16 (14) (2024) 6820–6836.
[18] I. Có Rives, A.Y.-A. Chen, A. Moore, Skin-based vaccination: a systematic mapping review of the types of vaccines and methods used and immunity and protection elicited in pigs, Vaccines 11 (2023) 450.
[19] M. Qin, G. Du, X. Sun, Recent advances in the noninvasive delivery of mRNA, Accounts Chem. Res. 54 (23) (2021) 4262–4271.
[20] S. Santra, M.R. Molla, Small molecule-based core and shell cross-linked nanoassemblies: from self-assembly and programmed disassembly to biological applications, Chem. Commun. 60 (84) (2024) 12101–12117.
[21] Q. Yin, W. Luo, V. Mallajosyula, Y. Bo, J. Guo, J. Xie, M. Sun, R. Verma, C. Li, C. M. Constantz, L.E. Wagar, J. Li, E. Sola, N. Gupta, C. Wang, O. Kask, X. Chen, X. Yuan, N.C. Wu, J. Rao, Y.-h. Chien, J. Cheng, B. Pulendran, M.M. Davis, A TLR7-nanoparticle adjuvant promotes a broad immune response against heterologous strains of influenza and SARS-CoV-2, Nat. Mater. 22 (3) (2023) 380–390.
[22] J. Weng, H. Yao, J. Wang, G. Li, Self-assembly morphology transition mechanism of similar amphiphilic molecules, Phys. Chem. Chem. Phys. 26 (1) (2024) 533–542.
[23] Y.Z. Liu, Y.N. Chen, Q. Sun, The dependence of hydrophobic interactions on the shape of solute surface, Molecules 29 (11) (2024).
[24] Y.C. Kim, C. Jarrahian, D. Zehrung, S. Mitragotri, M.R. Prausnitz, Delivery systems for intradermal vaccination, Curr. Top. Microbiol. Immunol. 351 (2012) 77–112.
[25] C. Möbs, M. Salheiser, F. Bleise, M. Witt, J.U. Mayer, Basophils control T cell priming through soluble mediators rather than antigen presentation, Front. Immunol. 13 (2023).
[26] C.M. Yuk, H.J. Park, B.-I. Kwon, S.J. Lah, J. Chang, J.-Y. Kim, K.-M. Lee, S.-H. Park, S. Hong, S.-H. Lee, Basophil-derived IL-6 regulates TH17 cell differentiation and CD4 T cell immunity, Sci. Rep. 7 (1) (2017) 41744.
[27] M. Sharma, J. Bayry, Basophils in autoimmune and inflammatory diseases, Nat. Rev. Rheumatol. 11 (3) (2015) 129–131.
[28] K. Chen, Y. Hao, M. Guzmán, G. Li, A. Cerutti, Antibody-mediated regulation of basophils: emerging views and clinical implications, Trends Immunol. 44 (6) (2023) 408–423.
[29] J. Zimmermann, S.D. van Haren, J. Diray-Arce, I.R. Adriawan, K. Wørzner, R. T. Krog, S. Guleed, T. Hu, R. Mortensen, J. Dietrich, S.M.Ø. Solbak, O. Levy, D. Christensen, G.K. Pedersen, Co-adjuvanting DDA/TDB liposomes with a TLR7 agonist allows for IgG2a/c class-switching in the absence of Th1 cells, npj Vaccines 8 (1) (2023) 189.
[30] W. Yu, L. Shen, J. Qi, T. Hu, Conjugation with loxoribine and mannan improves the immunogenicity of Mycobacterium tuberculosis CFP10-TB10.4 fusion protein, Eur. J. Pharm. Biopharm. 172 (2022) 193–202.
[31] I. Hardardottir, E.S. Olafsdottir, J. Freysdottir, Dendritic cells matured in the presence of the lycopodium alkaloid annotine direct T cell responses toward a Th2/Treg phenotype, Phytomedicine 22 (2) (2015) 277–282.
[32] A. Billiau, P. Matthys, Modes of action of Freund's adjuvants in experimental models of autoimmune diseases, J. Leukoc. Biol. 70 (6) (2001) 849–860.
[33] R. He, J. Zang, Y. Zhao, H. Dong, Y. Li, Nanotechnology-based approaches to promote lymph node targeted delivery of cancer vaccines, ACS Biomater. Sci. Eng. 8 (2) (2022) 406–423.
[34] Q. Li, Y. Yan, J. Liu, X. Huang, X. Zhang, C. Kirschning, H.C. Xu, P.A. Lang, U. Dittmer, E. Zhang, M. Lu, Toll-like receptor 7 activation enhances CD8+ T cell effector functions by promoting cellular glycolysis, Front. Immunol. 10 (2019).
[35] K. Shimoyama, K. Azuma, I. Nakamura, J. Oda, Prediction of the prognosis of patients with bacteremia caused by encapsulated organisms using spleen volume: a retrospective study, Acute Medicine & Surgery 8 (1) (2021) e698.
[36] Y.O. Alexandre, S.N. Mueller, Splenic stromal niches in homeostasis and immunity, Nat. Rev. Immunol. 23 (11) (2023) 705–719.
[37] E. Voltà-Durán, E. Parladé, N. Serna, A. Villaverde, E. Vázquez, U. Unzueta, Endosomal escape for cell-targeted proteins. Going out after going in, Biotechnol. Adv. (2023) 108103.
[38] J.L. Chollet, M.J. Jozwiakowski, K.R. Phares, M.J. Reiter, P.J. Roddy, H.J. Schultz, Q. Ta, M.A. Tomai, Development of a topically active imiquimod formulation, Pharmaceut. Dev. Technol. 4 1 (1999) 35–43.
[39] H. Zhu, K. Wang, Z. Wang, D. Wang, X. Yin, Y. Liu, F. Yu, W. Zhao, An efficient and safe MUC1-dendritic cell-derived exosome conjugate vaccine elicits potent cellular and humoral immunity and tumor inhibition in vivo, Acta Biomater. 138 (2022) 491–504.
[40] R. Lu, C. Groer, P.A. Kleindl, K.R. Moulder, A. Huang, J.R. Hunt, S. Cai, D.J. Aires, C. Berkland, M.L. Forrest, Formulation and preclinical evaluation of a toll-like receptor 7/8 agonist as an anti-tumoral immunomodulator, J. Contr. Release 306 (2019) 165–176.
[41] W. Yin, B. Deng, Z. Xu, H. Wang, F. Ma, M. Zhou, Y. Lu, J. Zhang, Formulation and evaluation of lipidized imiquimod as an effective adjuvant, ACS Infect. Dis. 9 (2) (2023) 378–387.